

AC impedance spectroscopy of pore reduced cements: Influence of contact resistance

D. E. MACPHEE, S. L. CORMACK
University of Aberdeen, Meston Walk Old Aberdeen AB24 3UE, UK
E-mail: de.macphee@abdn.ac.uk

D. C. SINCLAIR
Department of Engineering Materials, University of Sheffield, Mappin Street,
Sheffield S1 3JD, UK

Pore reduced cements (PRC) are used as a high resistance matrix for ac impedance studies on cement systems with impedance data being collected over a range of temperatures (–60 to ca. 20 °C) and electrode contact pressures (up to 72 MPa). The results show the presence of two arcs in the complex impedance plots, Z^* , at all measured temperatures. The low frequency (LF) arc is attributed to an ineffective electrical contact at the sample/electrode interface and although the high frequency (HF) arc is associated with the cement, its characteristics are also influenced by the contact resistance. Arrhenius plots show the activation energy for conductivity associated with the LF and HF elements to be the same indicating similar conduction mechanisms. Low and high frequency arcs are resolved only by the different geometric factors (conductive volumes) associated with the ineffective contact and the bulk cement specimen. © 2000 Kluwer Academic Publishers

1. Introduction

Several groups [1–3] have already reported data from ac impedance spectroscopy (ACIS) studies on cement pastes. We have reported ACIS data on pore reduced cement (PRC) [4–6], a high density product prepared by the simultaneous compaction of partially hydrated cement grains and partial removal of excess mixing water [7]. One advantage of using PRC for impedance studies is that the comparatively closed microstructures represent a higher electrical resistance than those of conventional Portland cement pastes so that within the accessible frequency range of standard laboratory instrumentation, two complete semi-circular features on a complex impedance plane plot (Z^* ; $-Z_{\text{imag}}$ vs Z_{real}) are generated for relatively young specimens, with the higher frequency intercept being at the origin. This is in contrast to the more conductive, conventional (unpressed) pastes, where, even at very long ages, only the lower frequency arc is complete, and the higher frequency arc is only partially complete.

Our previous interpretations of ACIS data have been based on an equivalent circuit proposed from a consideration of potential conductive pathways within the PRC microstructure [4]. It is accepted that the electrical microstructure may be quite different from the physical microstructure but the microstructural model was intended as a useful starting point. It was previously proposed [4, 5] that the two semi-circular features observed in the Z^* plots for PRC were due to two parallel RC elements (associated with isolated, fluid-filled porosity and cement hydration products) connected in

series. However, distinct differences in properties of samples cured under wet and dry conditions, coupled with an analysis of combined spectroscopic plots [6] of the imaginary components of the impedance, Z'' , and electric modulus, M'' , have shown that although a series type equivalent circuit may have been appropriate for modelling our reported data, it is now clear that one of the features, the low frequency arc, is extrinsic to the cement paste and is associated with the cement-electrode interface.

This paper reports on our experience from ac impedance spectroscopy, of various electrode-cement contacts on PRC. The spreading (or contact) resistance, associated with a series of point contacts between grains and the electrode surface, has been recognised in measurements on electroceramics [8] and we explore the influence of contact resistances on the high frequency response which we had previously assigned uniquely to the cement [4, 5]. Three different electrode types were studied:

- steel and brass, to highlight the point contacts between grains and the flat metal surface,
- a low melting point InGa alloy, which would be expected to flow into the surface imperfections of the cement, and
- carbon cloth, saturated in 0.2 M NaOH, chosen to utilise the penetration of the highly conductive alkaline solution into the cement surface with charge being collected by the carbon cloth.

We also examine the conduction process by assessing the temperature dependence of conductance for both the high and low frequency elements. The resulting Arrhenius plots provide activation energy information which we use to investigate the relationship between the contact resistance and the conductivity characteristics of the cement-electrode system.

2. Experimental

Pore reduced cements were prepared by mixing OPC with water at a water-cement ratio (w/c) of 0.35 and casting the paste into cylindrical perspex moulds. After about 3 hours under plastic sheet, the pastes were struck from the mould and pressed (to 200 MPa) in a pore fluid squeezer, during which excess mix water was removed so that the effective w/c was reduced to around 0.1. More details of PRC manufacture can be found elsewhere [7]. Resulting PRC cylinders measured approximately 45 mm in length and 42 mm diameter. Two separate sets of measurements were then undertaken:

(i) *Variable electrode pressure experiments*; Two separate means of attaching electrodes to the PRC cylinder were employed. (a) brass electrodes (area = 0.59 cm²) were positioned centrally onto the ends of a PRC cylinder and held in position by pressure. (b) either the low melting point alloy, InGa (60 : 40 mole ratio), or graphite, saturated in 0.2 M NaOH, was applied to the cylinder ends through a mask containing a 0.5 cm² hole, centrally positioned on the PRC cylinder. Electrical contact from the electrode to the impedance analyser was made through strips of gold foil which were insulated from the hydraulic press with small alumina tiles, except in the case of graphite, where connection was directly to the graphite. All electrodes were pressed against the cement to provide equivalent pressures in the range 9 to 72 MPa.

(ii) *Variable temperature experiments*; steel electrodes were embedded centrally in the ends of cement cylinders during PRC manufacture. Screws were located into the screw threads on each electrode so that crocodile clip attachments could be made. ACIS data were collected over a range of temperatures between -60°C and room temperature by placing the cement-electrode system into a beaker partially submerged in a dry-ice/acetone slush bath. Temperature was recorded by a thermometer in the beaker.

In both experiments, final connections to the impedance analyser were via crocodile clips and coaxial cable. A Hewlett Packard 4192A impedance analyser coupled to a BBC microcomputer was used to collect the data over the ranges of electrode-cement pressing pressures and temperatures; impedance measurements were made over the frequency range 5 Hz to 2 MHz with an applied voltage of 0.1 V.

3. Results and discussion

3.1. Effect of contact pressing pressure

Fig. 1 represents a schematic of the PRC-electrode system; the cement grains and their hydration products (containing water) are modelled as spheres. It is

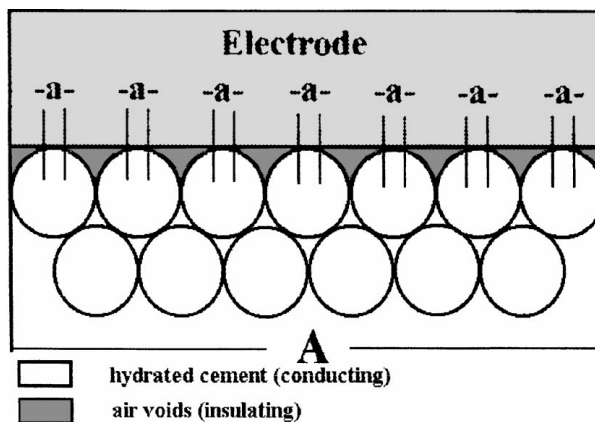


Figure 1 Schematic representation of the PRC-electrode interface. Cement is modelled by spheres and areas of point contact, $\Sigma(a) \ll A$, the area of the sample.

assumed that hydrated cement provides a conductive route between the bulk specimen and the electrode. In moist cured systems, porosity remains electrolyte-filled and a relatively complete conductive path across the entire electrode area can be expected. In dry conditions however, air voids form in the interfacial region as water is absorbed in hydration products. Consequently, the conductive hydration products can only have point contacts with the electrode [8]. The total contact area, i.e. the sum of the conducting point contacts, $\Sigma(a)$, therefore corresponds to an area which is very much less than the specimen area, A , at normal pressures. It would be expected that as pressure between the bulk material and the electrode is increased, the area of contact increases (assuming that there is some compressibility of the material), so that as pressure is increased, $\Sigma(a) \rightarrow A$.

The implications of this imperfect contact are that at normal pressures, two different conductivities can be calculated for a single material. This is because conductivity is geometry dependent, i.e. conductivity, $\sigma = \ell / RA$, where ℓ and A refer to length and cross sectional area respectively of the conductive element, and R is the resistance. For the bulk cement, A is the area of the sample but in the contact zone, $A = \Sigma(a)$ which is less than the sample area. Hwang *et al.* confirmed this by showing the pressure dependence of the contact resistance between alumina and gold [8]. A similar dependency was observed for the cement-electrode systems reported here and as indicated in Fig. 2 for the cement-brass system measured at room temperature.

Fig. 2 shows that portions of two semi-circular components are present for all pressures tested. At low pressure, the lower frequency (LF) element dominates the spectrum with the LF arc corresponding to a resistance of approximately 1 M Ω (less than half of this arc is shown on the scale of Fig. 2). The contribution of the higher frequency element (HF arc) is observed as a shoulder at low Z' values. The resistance corresponding to the LF contribution diminishes significantly as the applied pressure increases; at 72 MPa, this is reduced to less than 200 Ω and the HF arc becomes more prominent. A similar pressure dependence is observed with steel electrodes and this is indicative of the poor electrical contact at the electrode/cement interface.

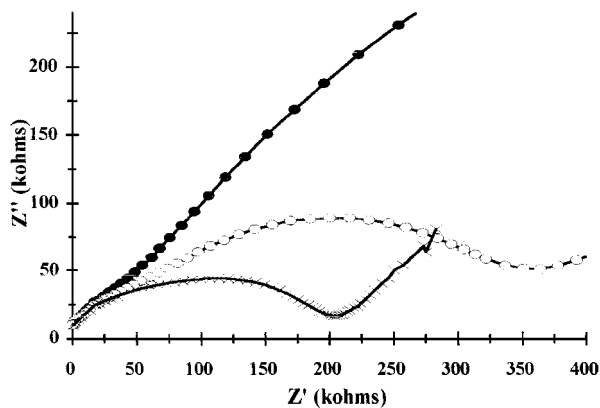


Figure 2 Z^* plot showing the effect of contact pressure (12 (●), 36 (○) or 72 (×) MNm^{-2}) at room temperature using brass contacts.

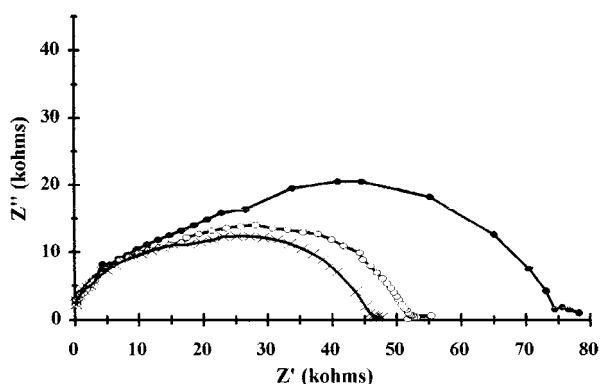


Figure 3 Z^* plot showing the effect of contact pressure (9 (●), 36 (○) or 54 (×) MNm^{-2}) for PRC using carbon/0.25 M NaOH contacts at room temperature.

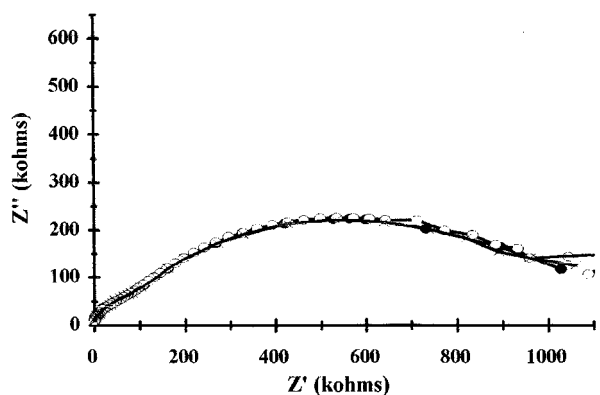


Figure 4 Z^* plot showing the effect of contact pressure (9 (●), 36 (○) or 54 (×) MNm^{-2}) for PRC using InGa contacts at room temperature.

Fig. 3 shows that the more penetrating NaOH solution coupled with the graphite provides a much more conductive contact (R_{LF} in the range 40–60 k Ω) but again, not ideal as indicated by the smaller, but still significant pressure dependence on cell resistance. Data for InGa/cement are shown in Fig. 4. While no significant pressure dependence is observed, the cell resistance remains high, ca. 1 M Ω indicating an ineffective contact. This is attributed to the poor wetting properties of the alloy on the cement surface.

It is more convenient to review electrode performance by interpolating data from the raw Z^* plots. The pressure dependence of resistance is shown in Fig. 5 for the brass, InGa and carbon/NaOH electrode sys-

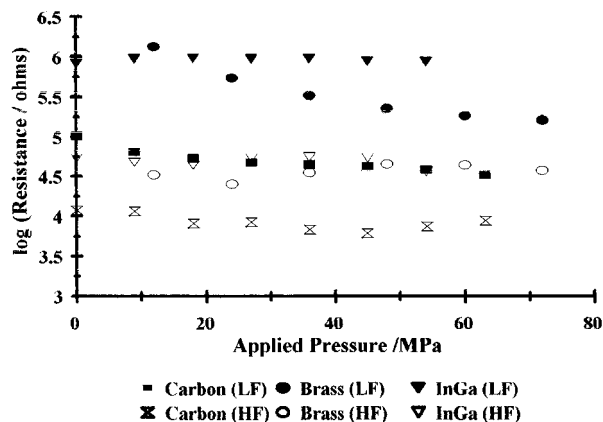


Figure 5 Effect of contact pressure on log(resistance) values derived from high (HF) and low frequency (LF) elements of Z^* plots for various contact types on PRC at room temperature.

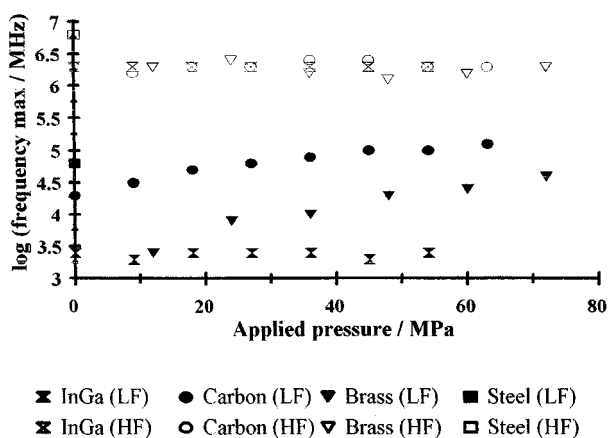


Figure 6 Effect of contact pressure on f_{max} for high (HF) and low frequency (LF) elements derived from spectroscopic plots for various contact types on PRC at room temperature.

tems. Both HF and LF data are presented. Resistances are estimated from the interpolated diameters of the semi-circular features with the real (Z') axis, whereby $R_T = R_{LF} + R_{HF}$ and R_T is the overall cell resistance. The relative insensitivity to pressure exhibited by the InGa and the carbon/NaOH systems can clearly be observed at both high and low frequencies but this is in contrast to the behaviour of the brass system. In this case, the resistance associated with the low frequency arc (R_{LF}) decreases gradually as pressure is increased but R_{HF} remains approximately constant. It is also important to note that while R_{HF} values over the experimental pressure range are similar for the brass and InGa systems, R_{HF} is almost an order of magnitude lower for the more conductive carbon/NaOH system. This indicates that the electrode contact problem also influences the HF component which was previously thought to be exclusively associated with the cement.

Spectroscopic data in the form of f_{max} , corresponding to the Z'' and M'' maxima when plotted against frequency, are presented in Fig. 6. Unlike resistance, f_{max} is geometry independent and Fig. 6 shows that for the high frequency arc, f_{max} is the same for all electrode systems studied. This is a most significant observation which confirms that the HF arc is derived from a feature of the system which does not involve

the cement-electrode contact, i.e. it is intrinsic to the cement. Despite the similarities in macroscopic cell geometry for all electrode systems studied, the observed difference in R_{HF} values extracted from the Z^* plots indicates that R_{HF} does not simply equate to R_{cement} . Instead, the ineffective contact gives a spreading resistance which alters the magnitude of the HF arc diameter [8] accounting for the different interpolated R_{HF} values.

3.2. Effect of temperature - Arrhenius plots

The activation energy for charge transport in a material is a very useful indicator of the conduction process occurring within the material. Activation energies can be obtained from log (conductance) vs reciprocal temperature plots, in which the gradient is equivalent to the term $-\Delta E_A/k$, where ΔE_A is the activation energy and k is Boltzmann's constant. It is interesting to note that graphs constructed for the data from both HF and LF arcs represent similar gradients (Figs 7 and 8) giving an E_A of approximately 0.5 eV. This indicates that the charge carrier and transport mechanism is the same for both the LF and HF elements. This also supports the idea that the LF arc is associated with a contact or spreading resistance. It is only the cross-sectional area through which conduction takes place that differentiates the HF and LF elements and this allows two arcs to

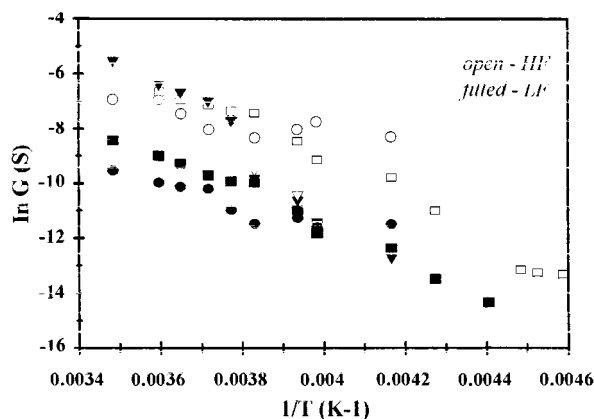


Figure 7 Arrhenius plots for HF (open) and LF (filled) arcs on Z^* plots using steel electrodes for PRC cooled immediately after pressing (∇) or after 2 (\square) and 5 (\circ) days.

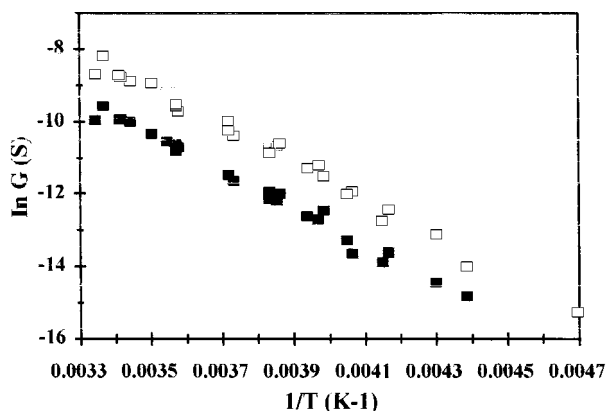


Figure 8 Arrhenius plots for HF (open) and LF (filled) arcs on Z^* plots using steel electrodes for PRC repeatedly cooled and warmed over a 66 hour period.

be observed in the Z^* plots. Given that the conductive medium is the same in both cases, i.e. cement paste, the same activation energy should be expected, however, the extracted conductance and resistance values obtained from Z^* plots, assuming an equivalent circuit of two parallel RC elements connected in series, will be different due to the different geometries associated with the two elements.

4. Conclusions

ac impedance data have been obtained for PRC with focus being centred on the importance of electrode contact with the specimen. Measurements have been made following application of a range of pressures onto the electrode-cement contact and temperature. Two semi-circular features are evident in all complex impedance plane plots. The present study has shown:

- a pressure dependence of the overall (or macroscopic) cell resistance, particularly for the LF element. This highlights an imperfect electrical contact similar to that reported by Hwang *et al.* [8] for gold on alumina in ceramic systems.
- based on spectroscopic plots of Z''_{max} and M''_{max} , that the HF element is associated with the bulk cement only.
- that the electrode contact influences R_{HF} data derived from Z^* plots.
- that both HF and LF elements have an activation energy of 0.5 eV, indicating similar conduction mechanisms for both features.

All of the data accumulated from this and our previous papers [4–6] point to the suggestion that both HF and LF arcs correspond to conductivity through cement, the HF arc being attributable to the bulk cement sample and the LF arc being associated with point contacts between the cement and the electrode. In the latter case, the cross sectional area for conduction is much smaller than that associated with the bulk cement so that techniques such as acIS, which are sensitive to geometry dependent parameters such as resistance, will distinguish two resistive regimes within the same material provided that the time constants, τ , where $\tau = RC$, are sufficiently different one another.

References

1. B. J. CHRISTENSEN, R. T. COVERDALE, R. A. OLSEN, S. J. FORD, E. J. GARBOCZI, H. M. JENNINGS and T. O. MASON, *J. Am. Ceram. Soc.* **77** (1994) 2789.
2. (a) W. J. MCCARTER, S. GARVIN and N. BOUZID, *J. Mat. Sci. Letts.* **11** (1988) 1056; (b) W. J. MCCARTER and S. GARVIN, *J. Phys. D: Appl. Phys.* **22** (1989) 1773.
3. Z. XU, P. GU, P. XIE and J. J. BEAUDOIN, *Cem. Concr. Res.* **23** (1993) 853.
4. D. E. MACPHEE, D. C. SINCLAIR and S. L. STUBBS, *J. Materials Science Letters* **15** (1996) 1566.
5. *Idem.*, *J. Am. Ceram. Soc.* **80** (1997) 2876.
6. S. L. CORMACK, D. E. MACPHEE and D. C. SINCLAIR, *Adv. Cements Research* **10** (1998) 151.
7. D. E. MACPHEE, *Advances in Cements Research* **3** (1990) 135.
8. J.-H. HWANG, K. S. KIRKPATRICK, T. O. MASON and E. J. GARBOCZI, *Solid State Ionics*, **98** (1997) 93.

Received 31 August 1999
and accepted 22 February 2000